Robotica (2005) volume 23, pp. 615–624. © 2005 Cambridge University Press
doi:10.1017/S0263574704001213 Printed in the United Kingdom

# Dynamic model and simulation of cooperative robots: a case study

Jorge Gudiño-Lau and Marco A. Arteaga*

*Departamento de Control y Robótica, División de Ingeniería Eléctrica de la Facultad de Ingeniería Universidad Nacional Autónoma de México México, D. F., 04510, (México)*

(Received in Final Form: October 1, 2004)

**SUMMARY**
Cooperative robots are usually required in flexible manufacturing systems or complex working environments. In particular, when an object under processing is too big or too heavy, a single robot may not be enough to handle it. Two or more manipulators are to be used in such a case. This paper presents the study of the dynamic equations for two industrial robots holding a rigid object. To this end, holonomic constraints are combined with the manipulators and object equations of motion to obtain the dynamic model of the whole system, which can be used for simulation purposes. Experimental results are presented to validate the theoretical results.

KEYWORDS: Modeling Cooperative robots; Simulation; Experimental results.

## I. INTRODUCTION

By cooperative robots we mean a group of manipulators holding a rigid object. Many benefits can be obtained by using them in industrial manufacturing. A typical example is in a flexible assembly, where the robots join two parts into a product. Cooperative manipulators can also be used in material handling, *e.g.* transporting objects beyond the load carrying capacity of a single robot. Furthermore, their employment allows to improve the quality of tasks in the manufacturer industry that require of great precision. On the other hand, cooperative robots are indispensable for skillful grasping and dexterous manipulation of objects. The dynamic analysis and control of such a system requires more sophisticated techniques compared with a single robot working scatteredly. Since the theory employed for cooperative robots is independent of their size, one can think of them as mechanical hands. The study of mechanical hands is important not only because these can be used as prosthetic devices for humans, but also because they increase considerably the manipulation capacity of a robot when substituting the usual gripper. However, the literature about experimental results on the modeling and simulation of systems of multiple manipulators holding a common object is rather sparse.

* Corresponding author. E-mail: arteaga@verona.fi-p.unam.mx

A dynamic analysis for a system of multiple manipulators is presented in Orin and Oh,[1] where the formalism of Newton–Euler for open chain mechanisms is extended for closed chain systems. Another approach widely used is the Euler–Lagrange method.[2] The equations of motion for each manipulator arm are developed in the Cartesian space and the impact of the closed chain is investigated when the held object is in contact with a rigid environment, for example the ground. Another general approach to obtain the dynamic model of a system of multiple robots is based on the estimation of the grasping matrix.[3–7] Here, the grasping matrix is used to couple the manipulators dynamics with that of the object, while this is modeled by the Newton–Euler formulation. The dynamic analysis for cooperative robots with flexible joints holding a rigid object is presented in Jankowski *et al*.[8]

In this paper, the dynamic model of two cooperative industrial manipulators holding a rigid body is presented, including force modeling. The interaction is described by the robot kinematics and the object equations of motion. Holonomic constraints are used to couple the kinematics and dynamics of the whole system. Also, it is explained how simulations can be carried out for Differential Algebraic Equations (DAE).

The paper is organized as follows. In Section II, the experimental test bed is presented. Section III gives the cooperative robots dynamic model, while Section IV shows simulation and experimental results. Conclusions are drawn in Section V.

## II. EXPERIMENTAL SYSTEM

The system under study is made up of two industrial robots and it is at the Laboratory for Robotics of the National University of Mexico (Fig. 1). They are the A465 and A255 of *CRS Robotics*. Even though the first one has six degrees of freedom and the second one five, only the first three joints of each manipulator are used in this case, while the rest of them are mechanically braked. Each joint is actuated by a direct current motor with optical encoders. Both manipulators have a crash protection device in the end effector and a force sensor installed on it; an aluminum finger is mounted on the sensor. The object is constituted by a melamine plastic box with dimensions $0.15\,\text{m} \times 0.15\,\text{m} \times 0.311\,\text{m}$ and weight $0.400\,\text{kg}$. The experiments are performed in a Pentium IV to 1.4 GHz personal computer with two

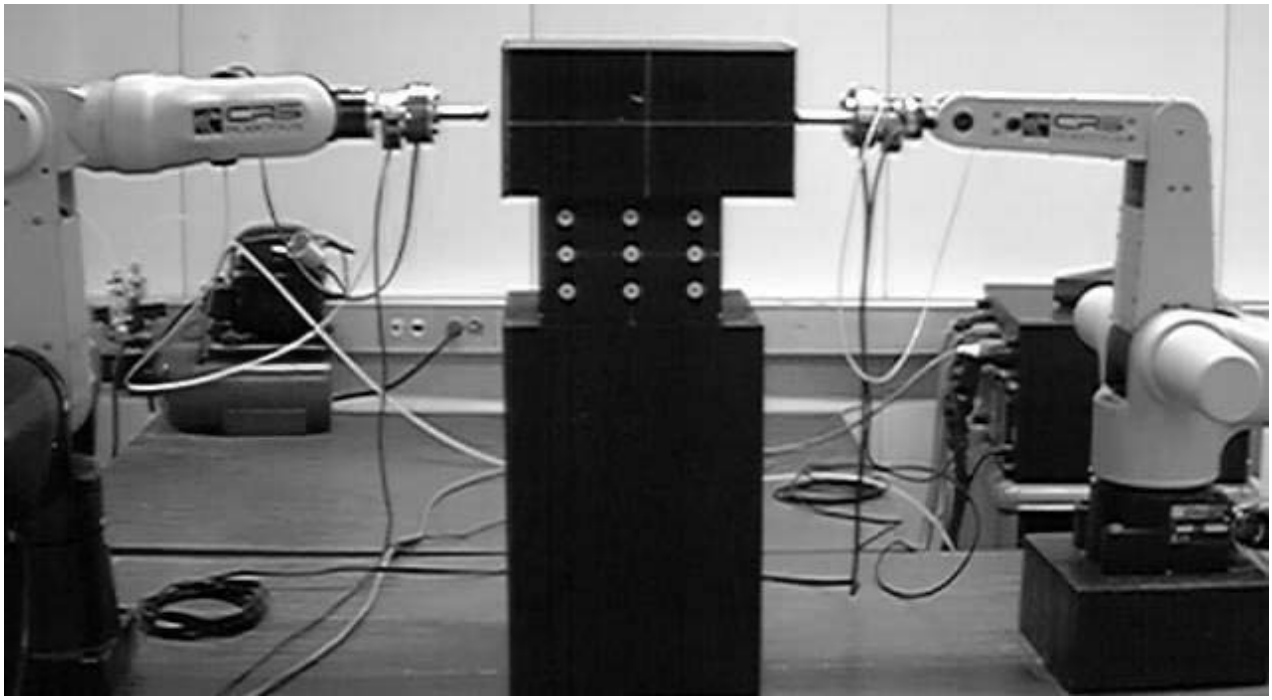

Fig. 1. Robots A465 and A255 of *CRS Robotics*.

PCI-FlexMotion-6C boards of *National Instruments*. The sampling time is of 9 ms. Controllers are programmed in the *LabWindows/CVI* software of *National Instruments*.

A schematic diagram of the robots holding an object is depicted in Fig. 2. The system variables are the generalized coordinates, velocities, and accelerations, as well as the contact forces exerted by the end effector on the common rigid object, and the generalized input forces (*i.e.* torques) acting on the joints.

To describe the kinematic relationships between the robots and the object, a stationary coordinate frame $C_0$ attached to the ground serves as reference frame, as shown in Fig. 2. An object coordinate frame $C_2$ is attached at the center of mass of the rigid object. The origin of the coordinate frame $C_1$ is located at the center of the end effector of robot A465. In the same way, the origin of the coordinate frame $C_3$ is located at the center of the end effector of robot A255. The coordinate frame $C_0$ has been considered to be the inertial frame of the whole system. ${}^0\boldsymbol{p}_2$ is the position vector of the object center of mass expressed in the coordinate system $C_0$. ${}^0\boldsymbol{p}_1$ and ${}^0\boldsymbol{p}_3$ are vectors that describe the position of the contact points between the end effectors of robots A465, A255 and the object, respectively, expressed in the coordinate system $C_0$.

## III. THE COOPERATIVE ROBOTS DYNAMIC MODEL

Consider the cooperative system with two robot arms shown in Fig. 1, each of them with $n_i = 3$ degrees of freedom and $m_i = 1$ constraints arising from the contact with the

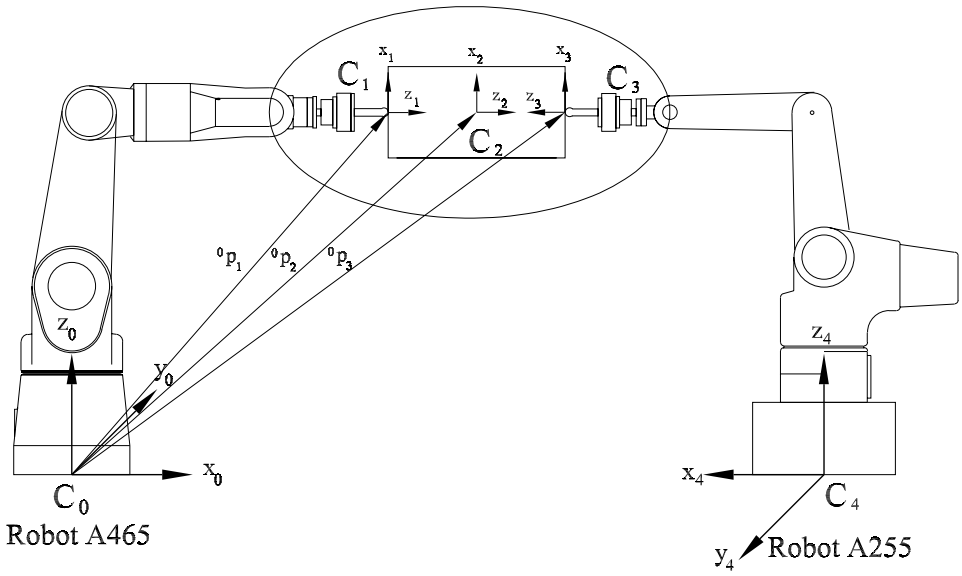


Fig. 2. Schematic diagram of robots holding an object.

https://doi.org/10.1017/S0263574704001213 Published online by Cambridge University Press

held object. Then, the total number of degrees of freedom is given by $n = \sum_{i=1}^{2} n_i$ with a total number of $m = \sum_{i=1}^{2} m_i$ constraints.

*III.1. Dynamic model with constraint motion*

The dynamic model for each individual manipulator, $i = 1, 2$, is obtained by the Lagrange's formulation as[9]

$$\begin{aligned} &\boldsymbol{H}_i(\boldsymbol{q}_i)\ddot{\boldsymbol{q}}_i + \boldsymbol{C}_i(\boldsymbol{q}_i, \dot{\boldsymbol{q}}_i)\dot{\boldsymbol{q}}_i + \boldsymbol{D}_i\dot{\boldsymbol{q}}_i + \boldsymbol{g}_i(\boldsymbol{q}_i) \\ &\quad = \boldsymbol{\tau}_i + \boldsymbol{J}_{\varphi_i}^{\mathrm{T}}(\boldsymbol{q}_i)\boldsymbol{\lambda}_i, \end{aligned} \tag{1}$$

where $\boldsymbol{q}_i \in \mathbb{R}^{n_i}$ is the vector of generalized joint coordinates, $\boldsymbol{H}_i(\boldsymbol{q}_i) \in \mathbb{R}^{n_i \times n_i}$ is the symmetric positive definite inertia matrix, $\boldsymbol{C}_i(\boldsymbol{q}_i, \dot{\boldsymbol{q}}_i)\dot{\boldsymbol{q}}_i \in \mathbb{R}^{n_i}$ is the vector of Coriolis and centrifugal torques, $\boldsymbol{g}_i(\boldsymbol{q}_i) \in \mathbb{R}^{n_i}$ is the vector of gravitational torques, $\boldsymbol{D}_i \in \mathbb{R}^{n_i \times n_i}$ is the positive semidefinite diagonal matrix accounting for joint viscous friction coefficients, $\boldsymbol{\tau}_i \in \mathbb{R}^{n_i}$ is the vector of generalized torques acting at the joints, and $\boldsymbol{\lambda}_i \in \mathbb{R}^{m_i}$ is the vector of Lagrange multipliers (physically represents the force applied at the contact point). $\boldsymbol{J}_{\varphi_i}^{\mathrm{T}}(\boldsymbol{q}_i)\boldsymbol{\lambda}_i$ represents the interaction of the rigid object with the two manipulators. $\boldsymbol{J}_{\varphi_i}(\boldsymbol{q}_i) = \nabla\boldsymbol{\varphi}_i(\boldsymbol{q}_i) \in \mathbb{R}^{m_i \times n_i}$ is assumed to be full rank in this paper. $\nabla\boldsymbol{\varphi}_i(\boldsymbol{q}_i)$ denotes the gradient of the object surface vector $\boldsymbol{\varphi}_i \in \mathbb{R}^{m_i}$, which maps a vector onto the normal plane at the tangent plane that arises at the contact point described by

$$\boldsymbol{\varphi}_i(\boldsymbol{q}_i) = \boldsymbol{0}. \tag{2}$$

Equation (2) is a geometrical constraint expressed in an analytical equation in which only position is involved and that does not depend explicitly of time $t$. Constraints of this forms are known as *holonomic constraints* (they are also classified as *sclero–holonomic*).

Note that equation (2) means that homogeneous constraints are being considered.[9] The complete system is subjected to 2 holonomic constraints given by

$$\boldsymbol{\varphi}(\boldsymbol{q}) = \boldsymbol{0}, \tag{3}$$

where $\boldsymbol{\varphi}(\boldsymbol{q}) = \boldsymbol{\varphi}(\boldsymbol{q}_1, \boldsymbol{q}_2) \in \mathbb{R}^m$. This means that the object being manipulated and the environment are modeled by the constraint (3). If the holonomic constraints are correctly calculated, then the object will remain hold. To have a better insight about the meaning of the constraint, consider rewriting the velocity vector $\dot{\boldsymbol{q}}_i$ as

$$\begin{aligned} \dot{\boldsymbol{q}}_i &= \dot{\boldsymbol{q}}_i + (\boldsymbol{J}_{\varphi_i}^{+}\boldsymbol{J}_{\varphi_i}\dot{\boldsymbol{q}}_i - \boldsymbol{J}_{\varphi_i}^{+}\boldsymbol{J}_{\varphi_i}\dot{\boldsymbol{q}}_i) \\ &= (\boldsymbol{I}_{n_i \times n_i} - \boldsymbol{J}_{\varphi_i}^{+}\boldsymbol{J}_{\varphi_i})\dot{\boldsymbol{q}}_i + \boldsymbol{J}_{\varphi_i}^{+}\boldsymbol{J}_{\varphi_i}\dot{\boldsymbol{q}}_i \\ &\triangleq \boldsymbol{Q}_i(\boldsymbol{q}_i)\dot{\boldsymbol{q}}_i + \boldsymbol{J}_{\varphi_i}^{+}(\boldsymbol{q}_i)\dot{\boldsymbol{p}}_i, \end{aligned} \tag{4}$$

where $\boldsymbol{J}_{\varphi_i}^{+} = \boldsymbol{J}_{\varphi_i}^{\mathrm{T}}(\boldsymbol{J}_{\varphi_i}\boldsymbol{J}_{\varphi_i}^{\mathrm{T}})^{-1} \in \mathbb{R}^{n_i \times m_i}$ stands for the Penrose's pseudoinverse and $\boldsymbol{Q}_i \in \mathbb{R}^{n_i \times n_i}$ satisfies $\mathrm{rank}(\boldsymbol{Q}_i) = n_i - m_i$. These two matrices are orthogonal, *i.e.* $\boldsymbol{Q}_i\boldsymbol{J}_{\varphi_i}^{+} = \boldsymbol{O}$ (and $\boldsymbol{Q}_i\boldsymbol{J}_{\varphi_i}^{\mathrm{T}} = \boldsymbol{O}$). Thus, the velocity vector $\dot{\boldsymbol{q}}_i$ has been split in two orthogonal subspaces. Let us analyze $\dot{\boldsymbol{p}}_i \triangleq \boldsymbol{J}_{\varphi_i}\dot{\boldsymbol{q}}_i \in \mathbb{R}^{m_i}$, which is the so called constrained velocity. In view of constraint (3), it holds

$$\sum_{i=1}^{l} \dot{\boldsymbol{p}}_i = \boldsymbol{0} \quad \text{and} \quad \sum_{i=1}^{l} \boldsymbol{p}_i = \sum_{i=1}^{l} \int_0^t \boldsymbol{J}_{\varphi_i}\dot{\boldsymbol{q}}_i \, \mathrm{d}t = \boldsymbol{0}, \tag{5}$$

where $l$ is the number of robots ($l = 2$). Since homogeneous constraints are being considered, it also holds from (2) that

$$\dot{\boldsymbol{p}}_i = \boldsymbol{0} \quad \text{and} \quad \boldsymbol{p}_i = \boldsymbol{0}, \tag{6}$$

for $i = 1, 2$. $\boldsymbol{p}_i$ is called the constrained position. As shown in Liu *et al.*,[10] if we consider homogeneous holonomic constraints we can write the constrained position, constrained velocity and constrained acceleration as

$$\boldsymbol{\varphi}_i(\boldsymbol{q}_i) = \boldsymbol{0} \tag{7}$$

$$\dot{\boldsymbol{\varphi}}_i(\boldsymbol{q}_i) = \boldsymbol{J}_{\varphi_i}(\boldsymbol{q}_i)\dot{\boldsymbol{q}}_i = \boldsymbol{0} \tag{8}$$

$$\ddot{\boldsymbol{\varphi}}_i(\boldsymbol{q}_i) = \boldsymbol{J}_{\varphi_i}(\boldsymbol{q}_i)\ddot{\boldsymbol{q}}_i + \dot{\boldsymbol{J}}_{\varphi}(\boldsymbol{q}_i)\dot{\boldsymbol{q}}_i = \boldsymbol{0}, \tag{9}$$

respectively. Recall that in our case $n_i = 3$, $n = 6$, $m_i = 1$, and $m = 2$, $i = 1, 2$.

*III.2. Dynamic model of the rigid object*

The motion of the two robot arms is dynamically coupled by the generalized contact forces interacting through the common rigid object. To describe this interaction, it is necessary to know the object dynamics. According to the free body diagram of Fig. 3, Newton's equation of motion are

$$\boldsymbol{m}_{\mathrm{o}}\ddot{\boldsymbol{x}}_{\mathrm{o}} - \boldsymbol{m}_{\mathrm{o}}\boldsymbol{g}_{\mathrm{o}} = \boldsymbol{f}_1 - \boldsymbol{f}_2, \tag{10}$$

where $\boldsymbol{m}_{\mathrm{o}} \in \mathbb{R}^{3\times3}$ is the diagonal mass matrix of the object, $\ddot{\boldsymbol{x}}_{\mathrm{o}} \in \mathbb{R}^3$ is the vector describing the translational acceleration of the center of mass of the rigid object, $\boldsymbol{f}_1 \in \mathbb{R}^3$ and $\boldsymbol{f}_2 \in \mathbb{R}^3$ are the forces exerted by the robots, and $\boldsymbol{g}_{\mathrm{o}} \in \mathbb{R}^3$ is a gravity vector. All vectors are expressed with reference to the inertial coordinate frame $C_0$. The contact forces vector are given by

$$\boldsymbol{f}_i = \boldsymbol{n}_i\lambda_i, \tag{11}$$

where $\boldsymbol{n}_i \in \mathbb{R}^3$ represents the direction of the force (normal to the constraint) and $\lambda_i \in \mathbb{R}$ given in (1).

*III.3. Assumptions to obtain the dynamic model*

The following assumptions are made to obtain the dynamic model for the cooperative system:

a) The end effectors (fingers) of the two robot arms are rigid.
b) The object is undeformable, and its absolute and relative position are known.
c) The kinematics of each robot is known.
d) Each manipulator is non–redundant and they do not reach any singularity.
e) The two robot arms system satisfy constraints (2) and (6) all time.

*III.4. Dynamic coupling*

The position, velocity and acceleration of the object center of mass with reference to the inertial coordinated frame are

https://doi.org/10.1017/S0263574704001213 Published online by Cambridge University Press

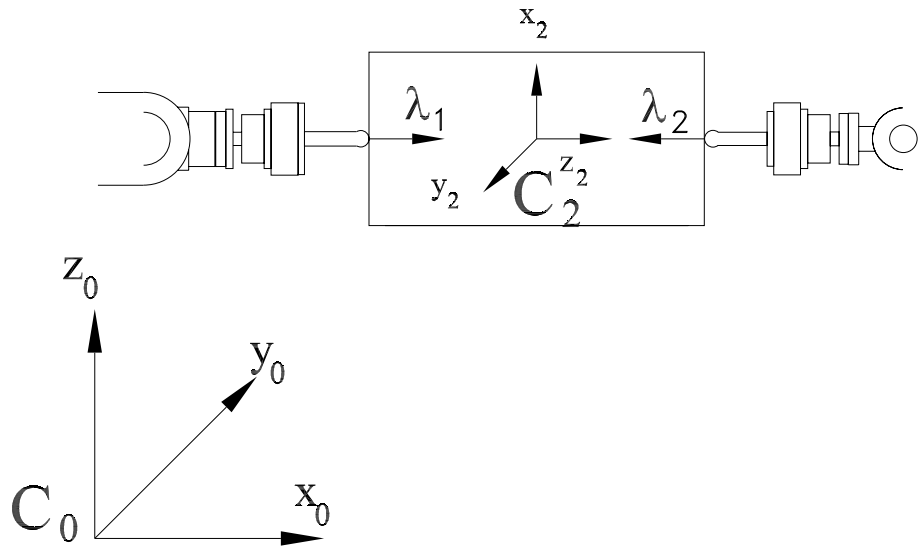


Fig. 3. Force free body diagram.

given in Cartesian coordinates by:

$$\boldsymbol{x}_{\mathrm{o}} = \boldsymbol{h}_i(\boldsymbol{q}_i) \tag{12}$$

$$\dot{\boldsymbol{x}}_{\mathrm{o}} = \boldsymbol{J}_{\mathrm{o}i}(\boldsymbol{q}_i)\dot{\boldsymbol{q}}_i \tag{13}$$

$$\ddot{\boldsymbol{x}}_{\mathrm{o}} = \boldsymbol{J}_{\mathrm{o}_i}(\boldsymbol{q}_i)\ddot{\boldsymbol{q}}_i + \dot{\boldsymbol{J}}_{\mathrm{o}}(\boldsymbol{q}_i)\dot{\boldsymbol{q}}_i, \tag{14}$$

respectively, with $i = 1, 2$. $\boldsymbol{h}_i(\boldsymbol{q}_i) \in \mathbb{R}^3$ is the forward kinematics of the center of mass of the object expressed in the coordinate system $C_0$, and $\boldsymbol{J}_{\mathrm{o}i} \in \mathbb{R}^{3\times 3}$ is the corresponding Jacobian matrix of $\boldsymbol{h}_i(\boldsymbol{q}_i)$. Substituting (14) into (10) yields

$$\boldsymbol{m}_{\mathrm{o}}\boldsymbol{J}_{\mathrm{o}_i}(\boldsymbol{q}_i)\ddot{\boldsymbol{q}}_i + \boldsymbol{m}_{\mathrm{o}}\dot{\boldsymbol{J}}_{\mathrm{o}_i}(\boldsymbol{q}_i)\dot{\boldsymbol{q}}_i - \boldsymbol{m}_{\mathrm{o}}\boldsymbol{g}_{\mathrm{o}} = \boldsymbol{f}_1 - \boldsymbol{f}_2. \tag{15}$$

Now, consider writing (1) as[6]

$$\begin{aligned}&\boldsymbol{H}_i(\boldsymbol{q}_i)\ddot{\boldsymbol{q}}_i + \boldsymbol{C}_i(\boldsymbol{q}_i, \dot{\boldsymbol{q}}_i)\dot{\boldsymbol{q}}_i + \boldsymbol{D}_i\dot{\boldsymbol{q}}_i + \boldsymbol{g}_i(\boldsymbol{q}_i)\\ &\quad = \boldsymbol{\tau}_i + \boldsymbol{J}_{\mathrm{a}_i}^{\mathrm{T}}(\boldsymbol{q}_i)\boldsymbol{f}_i.\end{aligned} \tag{16}$$

Note that

$$\boldsymbol{J}_{\varphi_i}^{\mathrm{T}}(\boldsymbol{q}_i) = \boldsymbol{J}_{\mathrm{a}_i}^{\mathrm{T}}(\boldsymbol{q}_i)\boldsymbol{n}_i, \tag{17}$$

in view of (11). $\boldsymbol{J}_{\mathrm{a}_i}(\boldsymbol{q}_i)$ is the manipulator analytical Jacobian. On the other hand, from (15) one gets

$$\boldsymbol{f}_1 = \boldsymbol{m}_{\mathrm{o}}\boldsymbol{J}_{\mathrm{o}_i}(\boldsymbol{q}_i)\ddot{\boldsymbol{q}}_i + \boldsymbol{m}_{\mathrm{o}}\dot{\boldsymbol{J}}_{\mathrm{o}_i}(\boldsymbol{q}_i)\dot{\boldsymbol{q}}_i - \boldsymbol{m}_{\mathrm{o}}\boldsymbol{g}_{\mathrm{o}} + \boldsymbol{f}_2. \tag{18}$$

Then, for $i = 1$ in (16) one gets

$$\begin{aligned}&\boldsymbol{H}_1(\boldsymbol{q}_1)\ddot{\boldsymbol{q}}_1 + \boldsymbol{C}_1(\boldsymbol{q}_1, \dot{\boldsymbol{q}}_1)\dot{\boldsymbol{q}}_1 + \boldsymbol{D}_1\dot{\boldsymbol{q}}_1 + \boldsymbol{g}_1(\boldsymbol{q}_1)\\ &\quad = \boldsymbol{\tau}_1 + \boldsymbol{J}_{\mathrm{a}_1}^{\mathrm{T}}(\boldsymbol{q}_1)\big(\boldsymbol{m}_{\mathrm{o}}\boldsymbol{J}_{\mathrm{o}_1}(\boldsymbol{q}_1)\ddot{\boldsymbol{q}}_1 + \boldsymbol{m}_{\mathrm{o}}\dot{\boldsymbol{J}}_{\mathrm{o}_1}(\boldsymbol{q}_1)\dot{\boldsymbol{q}}_1\\ &\qquad - \boldsymbol{m}_{\mathrm{o}}\boldsymbol{g}_{\mathrm{o}} + \boldsymbol{f}_2\big)\\ &\quad = \boldsymbol{\tau}_1 + \boldsymbol{J}_{\mathrm{a}_1}^{\mathrm{T}}(\boldsymbol{q}_1)\boldsymbol{m}_{\mathrm{o}}\boldsymbol{J}_{\mathrm{o}_1}(\boldsymbol{q}_1)\ddot{\boldsymbol{q}}_1 + \boldsymbol{J}_{\mathrm{a}_1}^{\mathrm{T}}(\boldsymbol{q}_1)\boldsymbol{m}_{\mathrm{o}}\dot{\boldsymbol{J}}_{\mathrm{o}_1}(\boldsymbol{q}_1)\dot{\boldsymbol{q}}_1\\ &\qquad - \boldsymbol{J}_{\mathrm{a}_1}^{\mathrm{T}}(\boldsymbol{q}_1)\boldsymbol{m}_{\mathrm{o}}\boldsymbol{g}_{\mathrm{o}} + \boldsymbol{J}_{\mathrm{a}_1}^{\mathrm{T}}(\boldsymbol{q}_1)\boldsymbol{f}_2,\end{aligned} \tag{19}$$

or

$$\begin{aligned}&\boldsymbol{\tau}_1 + \boldsymbol{J}_{\mathrm{a}_1}^{\mathrm{T}}(\boldsymbol{q}_1)\boldsymbol{f}_2\\ &\quad = \big(\boldsymbol{H}_1(\boldsymbol{q}_1) - \boldsymbol{J}_{\mathrm{a}_1}^{\mathrm{T}}(\boldsymbol{q}_1)\boldsymbol{m}_{\mathrm{o}}\boldsymbol{J}_{\mathrm{o}_1}(\boldsymbol{q}_1)\big)\ddot{\boldsymbol{q}}_1 + \big(\boldsymbol{C}_1(\boldsymbol{q}_1, \dot{\boldsymbol{q}}_1) + \boldsymbol{D}_1\\ &\qquad - \boldsymbol{J}_{\mathrm{a}_1}^{\mathrm{T}}(\boldsymbol{q}_1)\boldsymbol{m}_{\mathrm{o}}\dot{\boldsymbol{J}}_{\mathrm{o}_1}(\boldsymbol{q}_1)\big)\dot{\boldsymbol{q}}_1 + \boldsymbol{g}_1(\boldsymbol{q}_1) + \boldsymbol{J}_{\mathrm{a}_1}^{\mathrm{T}}(\boldsymbol{q}_1)\boldsymbol{m}_{\mathrm{o}}\boldsymbol{g}_{\mathrm{o}}.\end{aligned} \tag{20}$$

By defining

$$\boldsymbol{H}_{\mathrm{T}_1}(\boldsymbol{q}_1) \triangleq \boldsymbol{H}_1(\boldsymbol{q}_1) - \boldsymbol{J}_{\mathrm{a}_1}^{\mathrm{T}}(\boldsymbol{q}_1)\boldsymbol{m}_{\mathrm{o}}\boldsymbol{J}_{\mathrm{o}_1}(\boldsymbol{q}_1) \tag{21}$$

$$\boldsymbol{C}_{\mathrm{T}_1}(\boldsymbol{q}_1, \dot{\boldsymbol{q}}_1) \triangleq \boldsymbol{C}_1(\boldsymbol{q}_1, \dot{\boldsymbol{q}}_1) + \boldsymbol{D}_1 - \boldsymbol{J}_{\mathrm{a}_1}^{\mathrm{T}}(\boldsymbol{q}_1)\boldsymbol{m}_{\mathrm{o}}\dot{\boldsymbol{J}}_{\mathrm{o}_1}(\boldsymbol{q}_1) \tag{22}$$

$$\boldsymbol{g}_{\mathrm{T}_1}(\boldsymbol{q}_1) \triangleq \boldsymbol{g}_1(\boldsymbol{q}_1) + \boldsymbol{J}_{a_1}^{\mathrm{T}}(\boldsymbol{q}_1)\boldsymbol{m}_{\mathrm{o}}\boldsymbol{g}_{\mathrm{o}}, \tag{23}$$

one finally gets

$$\begin{aligned}&\boldsymbol{H}_{\mathrm{T}_1}(\boldsymbol{q}_1)\ddot{\boldsymbol{q}}_1 + \boldsymbol{C}_{\mathrm{T}_1}(\boldsymbol{q}_1, \dot{\boldsymbol{q}}_1)\dot{\boldsymbol{q}}_1 + \boldsymbol{g}_{\mathrm{T}_1}(\boldsymbol{q}_1)\\ &\quad = \boldsymbol{\tau}_1 + \boldsymbol{J}_{\mathrm{a}_1}^{\mathrm{T}}(\boldsymbol{q}_1)\boldsymbol{f}_2.\end{aligned} \tag{24}$$

In the same fashion, we make the analysis for the robot A255, to get

$$\begin{aligned}&\boldsymbol{H}_{\mathrm{T}_2}(\boldsymbol{q}_2)\ddot{\boldsymbol{q}}_2 + \boldsymbol{C}_{\mathrm{T}_2}(\boldsymbol{q}_2, \dot{\boldsymbol{q}}_2)\dot{\boldsymbol{q}}_2 + \boldsymbol{g}_{\mathrm{T}_2}(\boldsymbol{q}_2)\\ &\quad = \boldsymbol{\tau}_2 + \boldsymbol{J}_{\mathrm{a}_2}^{\mathrm{T}}(\boldsymbol{q}_2)\boldsymbol{f}_1,\end{aligned} \tag{25}$$

with

$$\boldsymbol{H}_{\mathrm{T}_2}(\boldsymbol{q}_2) \triangleq \boldsymbol{H}_2(\boldsymbol{q}_2) + \boldsymbol{J}_{\mathrm{a}_2}^{\mathrm{T}}(\boldsymbol{q}_2)\boldsymbol{m}_{\mathrm{o}}\boldsymbol{J}_{\mathrm{o}_2}(\boldsymbol{q}_2) \tag{26}$$

$$\boldsymbol{C}_{\mathrm{T}_2}(\boldsymbol{q}_2, \dot{\boldsymbol{q}}_2) \triangleq \boldsymbol{C}_2(\boldsymbol{q}_2, \dot{\boldsymbol{q}}_2) + \boldsymbol{D}_2 + \boldsymbol{J}_{\mathrm{a}_2}^{\mathrm{T}}(\boldsymbol{q}_2)\boldsymbol{m}_{\mathrm{o}}\dot{\boldsymbol{J}}_{\mathrm{o}_2}(\boldsymbol{q}_2) \tag{27}$$

$$\boldsymbol{g}_{\mathrm{T}_2}(\boldsymbol{q}_2) \triangleq \boldsymbol{g}_2(\boldsymbol{q}_2) - \boldsymbol{J}_{\mathrm{a}_2}^{\mathrm{T}}(\boldsymbol{q}_2)\boldsymbol{m}_{\mathrm{o}}\boldsymbol{g}_{\mathrm{o}}. \tag{28}$$

The dynamic models in (24)–(25) describe the motion of the entire closed chain, where each individual manipulator represents a subsystem coupled to the other one through kinematic and dynamic constraints.

https://doi.org/10.1017/S0263574704001213 Published online by Cambridge University Press

*III.5. Force modeling for cooperative robots*

A robot manipulator in free motion does not have geometric constraints; therefore, the dynamic model is described by Ordinary Differential Equations (ODE). When working with constrained motion, there appear holonomic constraints; for this reason, the dynamic model is described by Differential Algebraic Equations (DAE). To simulate contact forces, DAE's must be solved. First of all, from the dynamic model for cooperative robots (1), we obtain

$$\ddot{\boldsymbol{q}}_i = \boldsymbol{H}_i^{-1}(\boldsymbol{q}_i)\big(\boldsymbol{\tau}_i + \boldsymbol{J}_{\varphi_i}^{\mathrm{T}}(\boldsymbol{q}_i)\lambda_i - \boldsymbol{C}_i(\boldsymbol{q}_i, \dot{\boldsymbol{q}}_i)\dot{\boldsymbol{q}}_i - \boldsymbol{D}_i\dot{\boldsymbol{q}}_i - \boldsymbol{g}_i(\boldsymbol{q}_i)\big). \tag{29}$$

However, (7)–(9) must hold as well. Substituting the right hand side of (29) into (9) yields

$$\begin{aligned}\ddot{\boldsymbol{\varphi}}_i(\boldsymbol{q}_i) &= \boldsymbol{J}_{\varphi_i}(\boldsymbol{q}_i)\big[\boldsymbol{H}_i^{-1}(\boldsymbol{q}_i)\big(\boldsymbol{\tau}_i + \boldsymbol{J}_{\varphi_i}^{\mathrm{T}}(\boldsymbol{q}_i)\lambda_i - \boldsymbol{C}_i(\boldsymbol{q}_i, \dot{\boldsymbol{q}}_i)\dot{\boldsymbol{q}}_i \\ &\quad - \boldsymbol{D}_i\dot{\boldsymbol{q}}_i - \boldsymbol{g}_i(\boldsymbol{q}_i)\big)\big] + \dot{\boldsymbol{J}}_{\varphi_i}(\boldsymbol{q}_i)\dot{\boldsymbol{q}}_i \\ &= \boldsymbol{J}_{\varphi_i}(\boldsymbol{q}_i)\boldsymbol{H}_i^{-1}(\boldsymbol{q}_i)\boldsymbol{J}_{\varphi_i}^{\mathrm{T}}(\boldsymbol{q}_i)\lambda_i + \dot{\boldsymbol{J}}_{\varphi_i}(\boldsymbol{q}_i)\dot{\boldsymbol{q}}_i \\ &\quad + \boldsymbol{J}_{\varphi_i}(\boldsymbol{q}_i)\boldsymbol{H}_i^{-1}(\boldsymbol{q}_i)(\boldsymbol{\tau}_i - \boldsymbol{C}_i(\boldsymbol{q}_i, \dot{\boldsymbol{q}}_i)\dot{\boldsymbol{q}}_i \\ &\quad - \boldsymbol{D}_i\dot{\boldsymbol{q}}_i - \boldsymbol{g}_i(\boldsymbol{q}_i)) \\ &= \boldsymbol{0}.\end{aligned} \tag{30}$$

From the previous equation we obtain

$$\begin{aligned}\lambda_i = \big(\boldsymbol{J}_{\varphi_i}(\boldsymbol{q}_i)\boldsymbol{H}_i^{-1}(\boldsymbol{q})\boldsymbol{J}_{\varphi_i}^{\mathrm{T}}(\boldsymbol{q}_i)\big)^{-1}\,[\ddot{\boldsymbol{\varphi}}_i(\boldsymbol{q}_i) - \dot{\boldsymbol{J}}_{\varphi_i}(\boldsymbol{q}_i)\dot{\boldsymbol{q}}_i \\ - \boldsymbol{J}_{\varphi_i}(\boldsymbol{q}_i)\boldsymbol{H}_i^{-1}(\boldsymbol{q}_i)(\boldsymbol{\tau}_i - \boldsymbol{C}_i(\boldsymbol{q}_i, \dot{\boldsymbol{q}}_i)\dot{\boldsymbol{q}}_i - \boldsymbol{D}_i\dot{\boldsymbol{q}}_i - \boldsymbol{g}_i(\boldsymbol{q}_i))].\end{aligned} \tag{31}$$

The system described by (2), (6), (11), (24)–(25) and (31) could now be simulated as second order differential equations. However, the inclusion of the constraints in the form (31) does not guarantee the convergence of the contact velocity and position constraints to zero. This is because $\ddot{\boldsymbol{\varphi}}_i(\boldsymbol{q}_i) = 0$ represents a double integrator. Thus, any small difference of $\boldsymbol{\varphi}_i(\boldsymbol{q}_i)$ or $\dot{\boldsymbol{\varphi}}_i(\boldsymbol{q}_i)$ from zero in (7)–(9) will diverge. This problem has been successfully addressed by the constraint stabilization method in the solution of DAE's.[11] According to this approach, the constraints are asymptotically stabilized by using

$$\ddot{\boldsymbol{\varphi}}_i(\boldsymbol{q}_i) + 2\alpha_i\dot{\boldsymbol{\varphi}}_i(\boldsymbol{q}_i) + \beta_i\boldsymbol{\varphi}_i(\boldsymbol{q}_i) = \boldsymbol{0}, \tag{32}$$

instead of $\ddot{\boldsymbol{\varphi}}_i(\boldsymbol{q}_i) = \boldsymbol{0}$. $\alpha_i$ and $\beta_i$ are chosen appropriately to ensure the fast convergence of both the constraint position $\boldsymbol{\varphi}_i(\boldsymbol{q}_i)$ and velocity constraint $\dot{\boldsymbol{\varphi}}_i(\boldsymbol{q}_i)$ to zero (in case of offset). Equations (2), (6), (11), (24)–(25) and (31)–(32) fully describe the motion of the system to be simulated.

## IV. SIMULATION AND EXPERIMENTAL RESULTS

In this section, some simulation results are presented. To test the accuracy of the modeling approach, experimental results are carried out as well. To protect the manipulators of the cooperative system again possible damages, the position/force control approach given in Gudiño–Lau *et al.*[12] has been used for validation purposes. For the object equation of motion given in (10), it is $\boldsymbol{m}_{\mathrm{o}} = m_{\mathrm{obj}}\boldsymbol{I}$, $m_{\mathrm{obj}} = 0.400\,\mathrm{kg}$, and $\boldsymbol{g}_{\mathrm{o}}^{\mathrm{T}} = \{g_x\ g_y\ g_z\} = \{0\,0\,{-9.81}\,\mathrm{m/s^2}\}$. The object dimensions are $0.15\,\mathrm{m} \times 0.15\,\mathrm{m} \times 0.311\,\mathrm{m}$. In (32) one has $\alpha_i = 10$ and $\beta_i = 100$. The robots models are given in Appendix A.

The palm frame of the whole system is at the base of the robot A465, with its $x$–axis pointing towards the other manipulator. The task consists in lifting the object and pushing with a desired force, so that the constraints in Cartesian coordinates are simply given by

$$\varphi_i = x_i - b_i = 0, \tag{33}$$

for $i = 1, 2$ and $b_i$ a positive constant. The desired trajectories are given by

$$x_{\mathrm{d}_1} = 0.554[\mathrm{m}] \qquad x_{\mathrm{d}_2} = 0.865[\mathrm{m}] \tag{34}$$

$$y_{\mathrm{d}_{1,2}} = 0.05\sin(\omega(t - t_{\mathrm{i}}))[\mathrm{m}] \tag{35}$$

$$z_{\mathrm{d}_{1,2}} = (0.46 + 0.05\cos(\omega(t - t_{\mathrm{i}})))[\mathrm{m}]. \tag{36}$$

Note that the inverse kinematics of the manipulators has to be employed to compute $q_{\mathrm{d}_i}$. These trajectories are valid from an initial time $t_{\mathrm{i}} = 10\,\mathrm{s}$ to a final time $t_{\mathrm{f}} = 70\,\mathrm{s}$. Before $t_{\mathrm{i}}$ and after $t_{\mathrm{f}}$ the robots are in free motion. $\omega$ is a fifth order polynomial designed to satisfy $\omega(t_{\mathrm{i}}) = \omega(t_{\mathrm{f}}) = 0$. The derivatives of $\omega$ are also zero at $t_{\mathrm{i}}$ and $t_{\mathrm{f}}$. By choosing (34)–(36), the robots will make a circle in the $y$–$z$ plane. The only difference between the trajectories for robots A465 and A255 is the width of the object. Also, no force control is carried out until the manipulators are in the initial position to hold the object, at (0.554, 0, 0.510)[m] for the first manipulator and (0.865, 0, 0.510)[m] for the second one. The desired pushing forces are then given from $t = t_{\mathrm{i}} = 10\,\mathrm{s}$ to $t = t_{\mathrm{f}} = 70\,\mathrm{s}$ by

$$\begin{aligned} f_{\mathrm{d}x_{1,2}} &= 7.5(t - t_{\mathrm{i}})/5[\mathrm{N}] && t_{\mathrm{i}} \le t < 20\,\mathrm{s} \\ f_{\mathrm{d}x_{1,2}} &= 15 + 5\sin(3\pi(t - 20)/40)[\mathrm{N}] && 20 \le t < 60\,\mathrm{s} \\ f_{\mathrm{d}x_{1,2}} &= 15 - 7.5(t - 60)/5[\mathrm{N}] && 60 \le t < t_{\mathrm{f}}\,\mathrm{s} \end{aligned}$$

and $f_{\mathrm{d}y_{1,2}} = f_{\mathrm{d}z_{1,2}} = 0[\mathrm{N}]$. Note that, for simplicity, the desired forces are expressed in the base coordinate frame of each robot.

The control scheme has been programmed in a PC computer, whit sampling time 9 ms. The controller has also been digitalized for the simulation. The experiment lasts 80 s. The object is held at $t = 10\,\mathrm{s}$. Before, the robots are in free motion and the force control term of the algorithm given in Gudiño–Lau *et al.*[12] is not used, while from $t = 10\,\mathrm{s}$ to $t = 70\,\mathrm{s}$ it is switched on, *i.e.* the complete control–observer force scheme is employed only during this period of time. From $t = 70\,\mathrm{s}$ to $t = 80\,\mathrm{s}$ the robots go back to their initial positions in free motion. From $t = 10\,\mathrm{s}$ to $t = 15\,\mathrm{s}$ they begin pushing at their initial positions to hold the object, and from $t = 15\,\mathrm{s}$ to $t = 20\,\mathrm{s}$ they lift it to the position where the circle will be made. From $t = 20\,\mathrm{s}$ to $t = 60\,\mathrm{s}$ this is done while the desired force is changed for a sinus signal, as can be seen in Fig. 4. Note that our purpose is to show that simulation results of the constrained system are acceptable by using the approach described in Section III. For this reason, the

https://doi.org/10.1017/S0263574704001213 Published online by Cambridge University Press

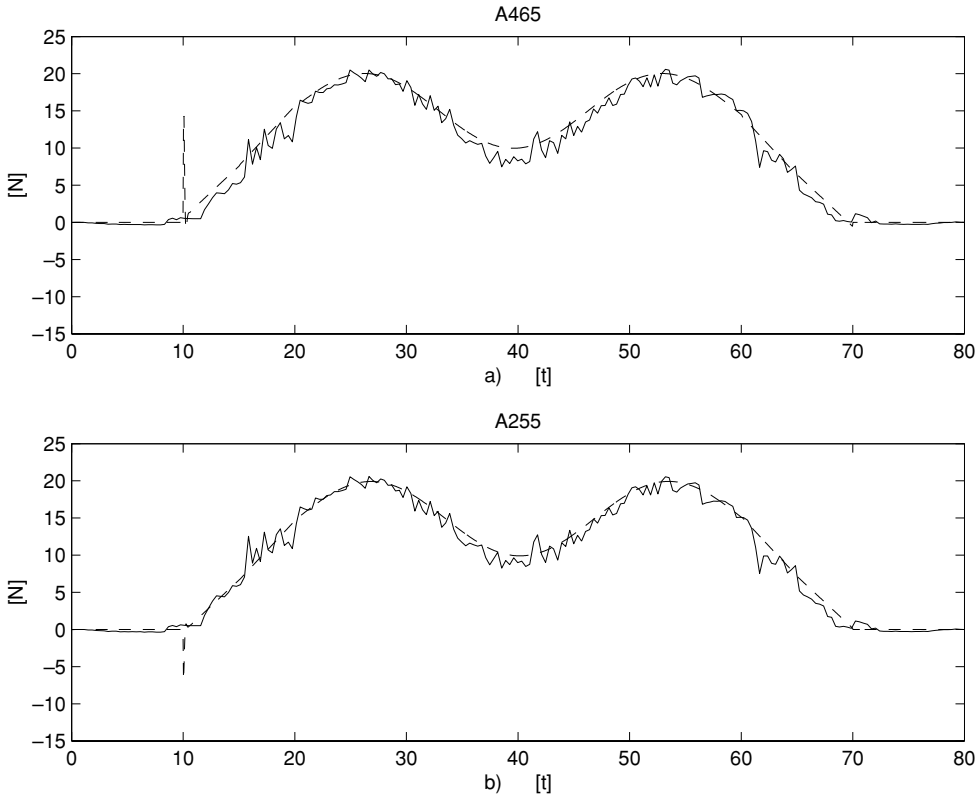


Fig. 4. Force measurements. a) $F_{x_1}$. b) $F_{x_2}$. —— experimental and - - - simulation.

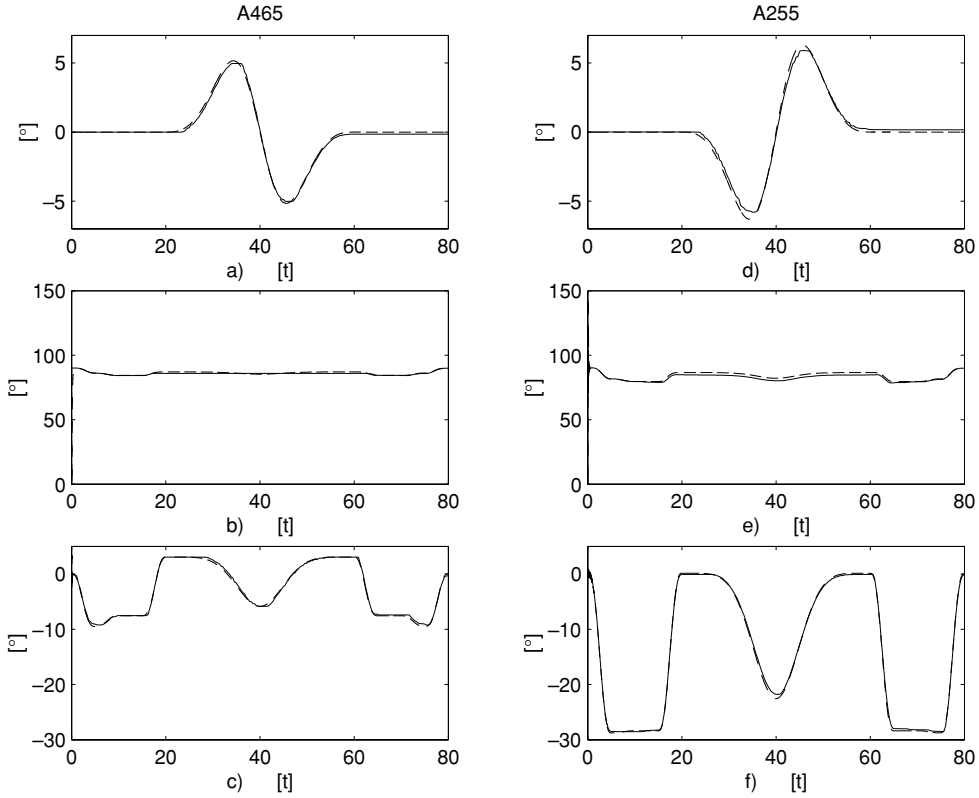


Fig. 5. Joint Coordinates a) $q_{11}$. b) $q_{12}$. c) $q_{13}$. d) $q_{21}$. e) $q_{22}$. f) $q_{23}$. —— experimental. - - - simulation.

https://doi.org/10.1017/S0263574704001213 Published online by Cambridge University Press

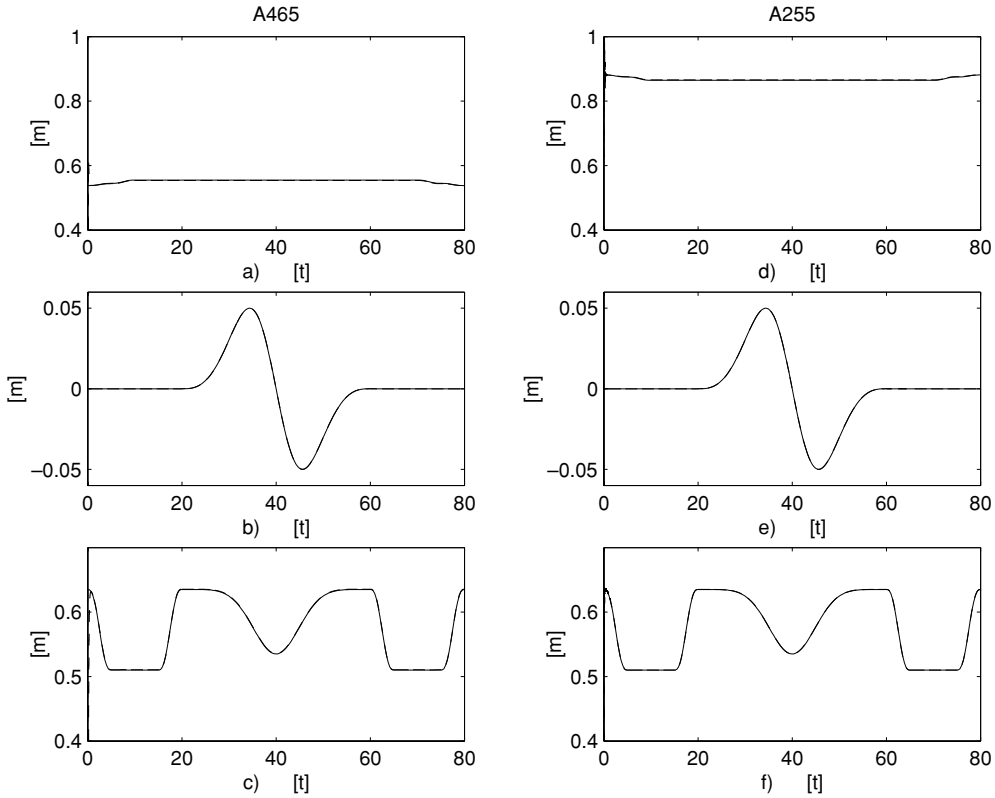


Fig. 6. Cartesian Coordinates a) $x_1$. b) $y_1$. c) $z_1$. d) $x_2$. e) $y_2$. f) $z_2$. —— experimental - - - simulation.

desired forces (or positions) are not shown. Only the real and simulated signals are presented. As can be seen, there is a good match. Of course, simulation results are free of noise. Note also that, since we have not proposed any special method to simulate the moment when the object is held, *i. e.*, when the robots change from free to constrained motion, there is a peak at $t = 10$ s in the simulation. From $t = 60$ s to $t = 65$ s the object is put down on the table and from $t = 65$ s to $t = 70$ s, the robots diminish pushing. Fig. 5 shows the simulation and experimental results of the joint coordinates, while Fig. 6 shows the results in Cartesian coordinates. As can be appreciated, the results are good in both cases.

## V. CONCLUSIONS

In this paper, we developed the model for two cooperative industrial robots holding a rigid object. The dynamic model for the manipulators is obtained independently from each other with the Lagrangian approach. Once the robots are holding the object, their joint variables are kinematically and dynamically coupled. These coupling equations are combined with the dynamic model of the object to obtain a mathematical description for the cooperative system.

Some experiments and simulations have been carried out to test the theoretical results. The overall outcome of the mathematical model compared with the real system can be considered good, which validates the approach used.

## Acknowledgments

This work is based on research supported by the **DGAPA–UNAM** under grants **IN106901** and **IN119003**, by the **CUDI** and scholarships by **CONACYT–Mexico** and **PROMEP–UdeC**.

## References

1. D. E. Orin and S. Y. Oh, "Control of force distribution in robotic mechanisms containing closed kinematics chains," *ASME Journal of Dynamic Systems, Measurement, and Control* **102**, 134–141 (1981).
2. T. Naniwa, S. Arimoto and K. Wada, "Learning and adaptive controls for coordination of multiple manipulators holding a geometrically constrained object," *IEEE International Conference on Intelligent Robots* (1997) **Vol. 1**, pp. 484–494.
3. A. Cole, P. Hsu and S. S. Sastry, "Dynamic control of sliding by robot hands for regrasping," *IEEE International Conference on Robotics and Automation* (1992) **Vol. 8**, pp. 42–52.
4. T. Y. Kuc, J. S. Lee and B. H. Park, "Learning control of cooperating robot manipulators handling an unknown object," *IEEE International Conference on System* (1995) **Vol. 3**, pp. 3339–3354.
5. G. F. Liu, J. Li and Z. X. Li, "Coordinated manipulation of objects by multifingered robotic hand in contact space and active joint space," *IEEE International Conference on Robotics and Automation* (2002) **Vol. 4**, pp. 3743–3748.
6. R. M. Murray, Z. Li and S. S. Sastry, *A Mathematical Introduction to Robotic Manipulation* (CRC Press, Boca Raton, Florida, U. S. A., 1994).
7. T. Yoshikawa and X. Z. Zheng, "Coordinated dynamic control for multiple robotic mechanisms handling an object," *IEEE/RSJ International Workshop on Intelligent Robots and Systems* (1991) pp. 315–320.
8. K. P. Jankowski, H. A. ElMaraghy and W. H. ElMaraghy, "Dynamic coordination of multiple robot arms with flexible joints," *Int. J. of Robotics Research* **12**, No. 6, 505–528 (1993).
9. V. Parra-Vega, A. Rodríguez-Ángeles, S. Arimoto and G. Hirzinger, "High precision constrained grasping with

https://doi.org/10.1017/S0263574704001213 Published online by Cambridge University Press

cooperative adaptive control," *Journal of Intelligent and Robotic System* **32**, 235–254 (2001).
10. Y. H. Liu, S. Arimoto, V. Parra–Vega and K. Kitagaki, "Decentralized adaptive control of multiple manipulators in cooperations," *International Journal of Control* **67**, No. 5, 649–673 (1997).
11. J. Baumgarte, "Stabilization of constraints and integrals of motion in dynamical systems," *Comput. Meth. Appl. Mech. Eng.* **1**, 1–16 (1972).
12. J. Gudiño–Lau, M. A. Arteaga–Pérez, L. A. Muñoz and V. Parra–Vega, "On the control of cooperative robots without velocity measurements," *IEEE Transactions on Control Systems Technology* **12**, No. 4, 600–608 (2004).
13. L. Sciavicco and B. Siciliano, *Modeling and Control of Robot Manipulators* (McGraw-Hill, Great Britain, 2000).

## APPENDIX A

This section presents the A465 and A255 robot models as well as the corresponding parameter values. The models used for implementation and simulation purposes include Coulomb friction term for both robots. The approach to model them can be found in any standard book for robotics.[13] Recall that only the first three degrees of freedom of each manipulator are being considered. Additionally, since the actuators are DC motors, their dynamics must be taken into account. Thus, for each manipulator (in free motion), one has

$$\begin{aligned}&\boldsymbol{H}_i(\boldsymbol{q}_i)\ddot{\boldsymbol{q}}_i + \boldsymbol{C}_i(\boldsymbol{q}_i, \dot{\boldsymbol{q}}_i)\dot{\boldsymbol{q}}_i + \boldsymbol{D}_i\dot{\boldsymbol{q}}_i + \boldsymbol{f}_{\mathrm{c}_i}(\dot{\boldsymbol{q}}_i) + \boldsymbol{g}_i(\boldsymbol{q}_i)\\ &\quad = \boldsymbol{D}_{\mathrm{n}_i}^{-1}\boldsymbol{D}_{\mathrm{k}_i}\boldsymbol{v}_i,\end{aligned} \tag{37}$$

where $\boldsymbol{f}_{\mathrm{c}_i}(\dot{\boldsymbol{q}}_i) \in \mathbb{R}^3$ represents the Coulomb friction term and $\boldsymbol{D}_{\mathrm{n}_i}$ and $\boldsymbol{D}_{\mathrm{k}_i} \in \mathbb{R}^{3\times 3}$ are to be defined later. The motors inertias are included in the matrix $\boldsymbol{H}_i(\boldsymbol{q}_i)$ so as to have a minimum set of parameters. The elements of matrices $\boldsymbol{H}_1(\boldsymbol{q}_1)$, $\boldsymbol{C}_1(\boldsymbol{q}_1, \dot{\boldsymbol{q}}_1)$, $\boldsymbol{f}_{\mathrm{c}_1}(\dot{\boldsymbol{q}}_1)$ and $\boldsymbol{g}_1(\boldsymbol{q}_1)$ of the model for Robot Arm A465 of *CRS Robotics* are computed as

$$\begin{aligned}
h_1(1,1) &= \mathrm{aux}_1\cdot p_1 + \mathrm{aux}_2\cdot p_2 + \mathrm{aux}_3\cdot p_3 + \mathrm{aux}_4\cdot p_4\\
&\quad + \mathrm{aux}_5\cdot p_5 + \mathrm{aux}_6\cdot p_6 + \mathrm{aux}_7\cdot p_7 + p_8\\
h_1(1,2) &= 0\\
h_1(1,3) &= 0\\
h_1(2,1) &= 0\\
h_1(2,2) &= \frac{1}{2}p_1 + p_2 + 2\mathrm{s}_3 p_3 + p_4 + p_9\\
h_1(2,3) &= \frac{1}{2}p_1 + p_2 + \mathrm{s}_3 p_3 + p_4 + p_5\\
h_1(3,1) &= 0\\
h_1(3,2) &= \frac{1}{2}p_1 + p_2 + \mathrm{s}_3 p_3 + p_4 + p_5\\
h_1(3,3) &= \frac{1}{2}p_1 + p_2 + p_4 + p_{10}\\
c_1(1,1) &= \mathrm{aux}_8\cdot p_3 + \mathrm{aux}_9\cdot p_5 - \frac{1}{2}\dot{q}_{12}\sin(2q_{12})p_6\\
&\quad + \frac{1}{2}\dot{q}_{12}\sin(2q_{12})p_7\\
c_1(1,2) &= \dot{q}_{11}\cos(2q_{12}+q_{13})p_3 + \frac{1}{2}\dot{q}_{11}\sin(2q_{12}+2q_{13})p_5\\
&\quad - \frac{1}{2}\dot{q}_{11}\sin(q_{12})p_6 + \frac{1}{2}\dot{q}_{11}\sin(2q_{12})p_7\\
c_1(1,3) &= \mathrm{aux}_{10}\cdot p_3 + \frac{1}{2}\dot{q}_{11}\sin(2q_{12}+2q_{13})p_5\\
c_1(2,1) &= -\dot{q}_{11}\cos(2q_{12}+q_{13})p_3 - \frac{1}{2}\dot{q}_{11}\sin(2q_{12}+2q_{13})p_5\\
&\quad + \frac{1}{2}\dot{q}_{11}\sin(2q_{12})p_6 - \frac{1}{2}\dot{q}_{11}\sin(2q_{12})p_7\\
c_1(2,2) &= \dot{q}_{13}\mathrm{c}_3 p_3\\
c_1(2,3) &= (\dot{q}_{12}\mathrm{c}_3 + \dot{q}_{13}\mathrm{c}_3)\,p_3\\
c_1(3,1) &= -\left(\frac{1}{2}\dot{q}_{11}\mathrm{c}_3 + \frac{1}{2}\dot{q}_{11}\cos(2q_{12}+q_{13})\right)p_3\\
&\quad - \frac{1}{2}\dot{q}_{11}\sin(2q_{12}+2q_{13})p_5\\
c_1(3,2) &= -\dot{q}_{12}\mathrm{c}_3 p_3\\
c_1(3,3) &= 0\\
f_{\mathrm{c}1}(1) &= p_{14}\mathrm{sgn}(\dot{q}_{11})\\
f_{\mathrm{c}1}(2) &= p_{15}\mathrm{sgn}(\dot{q}_{12})\\
f_{\mathrm{c}1}(3) &= p_{16}\mathrm{sgn}(\dot{q}_{13})\\
g_1(1) &= 0\\
g_1(2) &= p_{17}\mathrm{c}_2 + p_{21}\sin(q_{12}+q_{13})\\
g_1(3) &= p_{18}\sin(q_{12}+q_{13}).
\end{aligned}$$

Also, it is $\boldsymbol{D}_1 = \text{block diag}\,\{p_{11}\ p_{12}\ p_{13}\}$. $\boldsymbol{v}_1^{\mathrm{T}} = \{v_{11}\ v_{12}\ v_{13}\}$ is the input voltage. The motor dynamics data are $\boldsymbol{D}_{\mathrm{n}_1} = \text{block diag}\,\{\frac{1}{r_{11}^2}\ \frac{1}{r_{12}^2}\ \frac{1}{r_{13}^2}\}$ and $\boldsymbol{D}_{\mathrm{k}_1} = \text{block diag}\,\{\frac{K_{\mathrm{a}_{11}}}{R_{\mathrm{a}_{11}}r_{11}}\ \frac{K_{\mathrm{a}_{12}}}{R_{\mathrm{a}_{12}}r_{12}}\ \frac{K_{\mathrm{a}_{13}}}{R_{\mathrm{a}_{13}}r_{13}}\}$. Where $r$ stands for the gear ratio, $K_{\mathrm{a}}$ is the torque constant and $R_{\mathrm{a}}$ is the armature resistance. The associated values are $r_{11} = r_{12} = r_{13} = 100$, $K_{\mathrm{a}_{11}} = K_{\mathrm{a}_{12}} = K_{\mathrm{a}_{13}} = 0.1424$ Nm/A and $R_{\mathrm{a}_{11}} = R_{\mathrm{a}_{12}} = R_{\mathrm{a}_{13}} = 0.84\Omega$.

The elements of the corresponding matrices for the Robot Arm A255 are given by

$$\begin{aligned}
h_2(1,1) &= \cos(2q_{22})\bar{p}_1 + (2\mathrm{c}_5 + 2\mathrm{c}_6)\,\bar{p}_2 + \bar{p}_3\\
h_2(1,2) &= 0\\
h_2(1,3) &= 0\\
h_2(2,1) &= 0\\
h_2(2,2) &= \bar{p}_4\\
h_2(2,3) &= \cos(q_{22}-q_{23})\bar{p}_5\\
h_2(3,1) &= 0\\
h_2(3,2) &= \cos(q_{22}-q_{23})\bar{p}_5\\
h_2(3,3) &= \bar{p}_6\\
c_2(1,1) &= -\dot{q}_{22}\sin(2q_{22})\bar{p}_1 - (\mathrm{s}_5\dot{q}_{22} + \mathrm{s}_6\dot{q}_{23})\,\bar{p}_2\\
c_2(1,2) &= -\dot{q}_{21}\sin(2q_{22})\bar{p}_1 - \dot{q}_{21}\mathrm{s}_5\bar{p}_2
\end{aligned}$$

https://doi.org/10.1017/S0263574704001213 Published online by Cambridge University Press

Table I. Physical parameters of robot arm A465.

| | | | | |
|---|---|---|---|---|
| $p_1 = 0.0055\,\mathrm{kg\,m^2}$ | $p_2 = 0.0080\,\mathrm{kg\,m^2}$ | $p_3 = 0.0024\,\mathrm{kg\,m^2}$ | $p_4 = 0.0118\,\mathrm{kg\,m^2}$ | $p_5 = 0.0041\,\mathrm{kg\,m^2}$ |
| $p_6 = 0.0009\,\mathrm{kg\,m^2}$ | $p_7 = 0.0007\,\mathrm{kg\,m^2}$ | $p_8 = 2.0007\,\mathrm{kg\,m^2}$ | $p_9 = 11.800\,\mathrm{kg\,m^2}$ | $p_{10} = 2.8000\,\mathrm{kg\,m^2}$ |
| $p_{11} = 25.000\,\mathrm{N\,m\,s}$ | $p_{12} = 35.000\,\mathrm{N\,m\,s}$ | $p_{13} = 36.000\,\mathrm{N\,m\,s}$ | $p_{14} = 0.2000\,\mathrm{N\,m}$ | $p_{15} = 2.5000\,\mathrm{N\,m}$ |
| $p_{16} = 2.5000\,\mathrm{N\,m}$ | $p_{17} = 22.000\,\mathrm{N\,m}$ | $p_{18} = 11.000\,\mathrm{N\,m}$ | | |

Table II. Physical parameters of robot arm A255.

| | | | | |
|---|---|---|---|---|
| $\bar{p}_1 = 0.2500\,\mathrm{kg\,m^2}$ | $\bar{p}_2 = 0.0500\,\mathrm{kg\,m^2}$ | $\bar{p}_3 = 0.5750\,\mathrm{kg\,m^2}$ | $\bar{p}_4 = 1.1000\,\mathrm{kg\,m^2}$ | $\bar{p}_5 = 0.0300\,\mathrm{kg\,m^2}$ |
| $\bar{p}_6 = 0.5700\,\mathrm{kg\,m^2}$ | $\bar{p}_7 = 3.2000\,\mathrm{N\,m\,s}$ | $\bar{p}_8 = 1.8000\,\mathrm{N\,m\,s}$ | $\bar{p}_9 = 1.2000\,\mathrm{N\,m\,s}$ | $\bar{p}_{10} = 0.0150\,\mathrm{N\,m}$ |
| $\bar{p}_{11} = 0.8000\,\mathrm{N\,m}$ | $\bar{p}_{12} = 0.7000\,\mathrm{N\,m}$ | $\bar{p}_{13} = 0.0001\,\mathrm{N\,m}$ | $\bar{p}_{14} = 1.8000\,\mathrm{N\,m}$ | |

$$
\begin{aligned}
c_2(1,3) &= -\mathrm{s}_6\dot{q}_{21}\bar{p}_2\\
c_2(2,1) &= \dot{q}_{21}\sin(2q_{22})\bar{p}_1 + \dot{q}_{21}\mathrm{s}_5\bar{p}_2\\
c_2(2,2) &= 0\\
c_2(2,3) &= \sin(q_{22}-q_{23})\dot{q}_{23}\bar{p}_5\\
c_2(3,1) &= \mathrm{s}_6\dot{q}_{21}\bar{p}_2\\
c_2(3,2) &= -\sin(q_{22}-q_{23})\dot{q}_{22}\bar{p}_5\\
c_2(3,3) &= 0\\
f_{c2}(1) &= \bar{p}_{10}\mathrm{sgn}(\dot{q}_{21})\\
f_{c2}(2) &= \bar{p}_{11}\mathrm{sgn}(\dot{q}_{22})\\
f_{c2}(3) &= \bar{p}_{12}\mathrm{sgn}(\dot{q}_{23})\\
g_2(1) &= 0\\
g_2(2) &= \bar{p}_{13}\mathrm{c}_5\\
g_2(3) &= \bar{p}_{14}\mathrm{c}_6.
\end{aligned}
$$

For this robot one has $\boldsymbol{D}_2 = \text{block diag}\,\{\bar{p}_7\,\bar{p}_8\,\bar{p}_9\}$. The input voltages vector is given by $\boldsymbol{v}_2^{\mathrm{T}} = \{v_{21}\,v_{22}\,v_{23}\}$. The motor dynamics data are $\boldsymbol{D}_{\mathrm{n}_2} = \text{block diag}\,\{\frac{1}{r_{21}^2}\,\frac{1}{r_{22}^2}\,\frac{1}{r_{23}^2}\}$ and $\boldsymbol{D}_{\mathrm{k}_2} = \text{block diag}\,\{\frac{K_{\mathrm{a}_{21}}}{R_{\mathrm{a}_{21}}r_{21}}\,\frac{K_{\mathrm{a}_{22}}}{R_{\mathrm{a}_{22}}r_{22}}\,\frac{K_{\mathrm{a}_{23}}}{R_{\mathrm{a}_{23}}r_{23}}\}$. With $r_{21} = r_{22} = r_{23} = 72$, $K_{\mathrm{a}_{21}} = K_{\mathrm{a}_{22}} = K_{\mathrm{a}_{23}} = 0.0657\,\mathrm{Nm/A}$ and $R_{\mathrm{a}_{21}} = R_{\mathrm{a}_{22}} = R_{\mathrm{a}_{23}} = 2.40\Omega$. Note that in the model of both robots we could have chosen the parameters in a different fashion to have a smaller set. However, we made the definitions according to the computation of the inertia of the links. The elements of the analytical Jacobian $\boldsymbol{J}_{\mathrm{a}1}(\boldsymbol{q}_1)$ of robot A465 are given by

$$j_{\mathrm{a}1}(1,1) = -a_{12}s_1c_2 - (d_{13}+d_{14})s_1\sin(q_{12}+q_{13}) \quad (38)$$

$$j_{\mathrm{a}1}(1,2) = -a_{12}c_1s_2 + (d_{13}+d_{14})c_1\cos(q_{12}+q_{13}) \quad (39)$$

$$j_{\mathrm{a}1}(1,3) = (d_{13}+d_{14})c_1\cos(q_{12}+q_{13}) \quad (40)$$

$$j_{\mathrm{a}1}(2,1) = a_{12}c_1c_2 + (d_{13}+d_{14})c_1\sin(q_{12}+q_{13}) \quad (41)$$

$$j_{\mathrm{a}1}(2,2) = -a_{12}s_1s_2 + (d_{13}+d_{14})s_1\cos(q_{12}+q_{13}) \quad (42)$$

$$j_{\mathrm{a}1}(2,3) = (d_{13}+d_{14})s_1\cos(q_{12}+q_{13}) \quad (43)$$

$$j_{\mathrm{a}1}(3,1) = 0 \quad (44)$$

$$j_{\mathrm{a}1}(3,2) = a_{12}c_2 + (d_{13}+d_{14})\sin(q_{12}+q_{13}) \quad (45)$$

$$j_{\mathrm{a}1}(3,3) = (d_{13}+d_{14})\sin(q_{12}+q_{13}), \quad (46)$$

and those of $\boldsymbol{J}_{\mathrm{a}2}(\boldsymbol{q}_2)$ are:

$$j_{\mathrm{a}2}(1,1) = -a_{22}s_4c_5 - a_{23}s_4c_6 - d_{24}s_4 \quad (47)$$

$$j_{\mathrm{a}2}(1,2) = -a_{22}c_4s_5 \quad (48)$$

$$j_{\mathrm{a}2}(1,3) = -a_{23}c_4s_6 \quad (49)$$

$$j_{\mathrm{a}2}(2,1) = a_{22}c_4c_5 + a_{23}c_4c_6 + d_{24}c_4 \quad (50)$$

$$j_{\mathrm{a}2}(2,2) = -a_{22}s_4s_5 \quad (51)$$

$$j_{\mathrm{a}2}(2,3) = -a_{23}s_4s_6 \quad (52)$$

$$j_{\mathrm{a}2}(3,1) = 0 \quad (53)$$

$$j_{\mathrm{a}2}(3,2) = a_{22}c_5 \quad (54)$$

$$j_{\mathrm{a}2}(3,3) = a_{23}c_6. \quad (55)$$

The constraint Jacobian matrix $\boldsymbol{J}_{\varphi_1}(\boldsymbol{q}_1)$ of the robot arm A465 is:

$$\boldsymbol{J}_{\varphi_1}^{\mathrm{T}}(\boldsymbol{q}_1) = \begin{bmatrix} -a_{12}s_1c_2 - (d_{13}+d_{14})s_1\sin(q_{12}+q_{13}) \\ -a_{12}c_1s_2 + (d_{13}+d_{14})c_1\cos(q_{12}+q_{13}) \\ (d_{13}+d_{14})c_1\cos(q_{12}+q_{13}) \end{bmatrix}, \quad (56)$$

and the constraint Jacobian matrix $\boldsymbol{J}_{\varphi_2}(\boldsymbol{q}_2)$ of the robot arm A255 is:

$$\boldsymbol{J}_{\varphi_2}^{\mathrm{T}}(\boldsymbol{q}_2) = \begin{bmatrix} -a_{22}s_4c_5 - a_{23}s_4c_6 - d_{24}s_4 \\ -a_{22}c_4s_5 \\ -a_{23}c_4s_6 \end{bmatrix}. \quad (57)$$

Note that, for simplicity, both $\boldsymbol{J}_{\mathrm{a}2}(\boldsymbol{q}_2)$ and $\boldsymbol{J}_{\varphi_2}(\boldsymbol{q}_2)$ are expressed with respect with an inertial system fixed at the base of robot A255.

Tables I and II show the parameter values, and Tables III and IV the auxiliary variables for both robots. The parameters for the different Jacobian matrices are presented in Table V.

Table III. Auxiliary definitions.

| | |
|---|---|
| $\mathrm{s}_1 = \sin(q_{11})$ | $\mathrm{c}_1 = \cos(q_{11})$ |
| $\mathrm{s}_2 = \sin(q_{12})$ | $\mathrm{c}_2 = \cos(q_{12})$ |
| $\mathrm{s}_3 = \sin(q_{13})$ | $\mathrm{c}_3 = \cos(q_{13})$ |
| $\mathrm{s}_4 = \sin(q_{21})$ | $\mathrm{c}_4 = \cos(q_{21})$ |
| $\mathrm{s}_5 = \sin(q_{22})$ | $\mathrm{c}_5 = \cos(q_{22})$ |
| $\mathrm{s}_6 = \sin(q_{23})$ | $\mathrm{c}_6 = \cos(q_{23})$ |

https://doi.org/10.1017/S0263574704001213 Published online by Cambridge University Press

Table IV. Auxiliary variables in the model of the robot arm A465.

$\text{aux}_1 = \frac{3}{4} + \frac{1}{4}\cos(2q_{12} + 2q_{13})$
$\text{aux}_2 = \frac{1}{4} - \frac{1}{2}\cos(2q_{12} + 2q_{13})$
$\text{aux}_3 = \text{s}_3 + \sin(2q_{12} + q_{13})$
$\text{aux}_4 = \frac{1}{2} + \frac{1}{2}\cos(2q_{12} + 2q_{13})$
$\text{aux}_5 = \frac{1}{2} - \frac{1}{2}\cos(2q_{12} + 2q_{13})$
$\text{aux}_6 = \frac{1}{2} + \frac{1}{2}\cos(2q_{12})$
$\text{aux}_7 = \frac{1}{2} - \frac{1}{2}\cos(2q_{12})$
$\text{aux}_8 = [\dot{q}_{12}\cos(2q_{12} + q_{13}) + \frac{1}{2}\dot{q}_{13}\text{c}_3 + \frac{1}{2}\dot{q}_{13}\cos(2q_{12} + q_{13})]\frac{1}{\text{seg}}$
$\text{aux}_9 = [\frac{1}{2}\dot{q}_{13}\sin(2q_{12} + 2q_{13}) + \frac{1}{2}\dot{q}_{12}\sin(2q_{12} + 2q_{13})]\frac{1}{\text{seg}}$
$\text{aux}_{10} = [\frac{1}{2}\dot{q}_{11}\text{c}_3 + \frac{1}{2}\dot{q}_{11}\cos(2q_{12} + q_{13})]\frac{1}{\text{seg}}$

Table V. Data of the different Jacobian matrices.

| Robot arm A465 | Robot arm A255 |
|---|---|
| $d_{11} = 0.330$ [m] | $d_{21} = 0.381$ [m] |
| $a_{12} = 0.305$ [m] | $a_{22} = 0.254$ [m] |
| $d_{13} = 0.330$ [m] | $a_{23} = 0.254$ [m] |
| $d_{14} = 0.208$ [m] | $d_{24} = 0.183$ [m] |

https://doi.org/10.1017/S0263574704001213 Published online by Cambridge University Press